بسم الله الرحمن الرحيم

Tensor Decomposition For Colour Image Segmentation Of Burn Wounds

نیلوفر پورهروی
مارال محمود علی نژاد
استاژر
فروردین 1400

- RESULT AND DISCUSSION

- Figure 3 shows a burn image of 1330*1925*3 pixels of a pediatrics patient with a burn wound located on the right hand assessed 96 hours after the burn injury. The acquired RGB image was converted into the CIELab colour space with standard D65 illuminant and its components were filtered in the frequency domain with Gaussian filters, keeping the 99% of the power spectrum of the zero-padded discrete Fourier transforms of them (see Fig4).

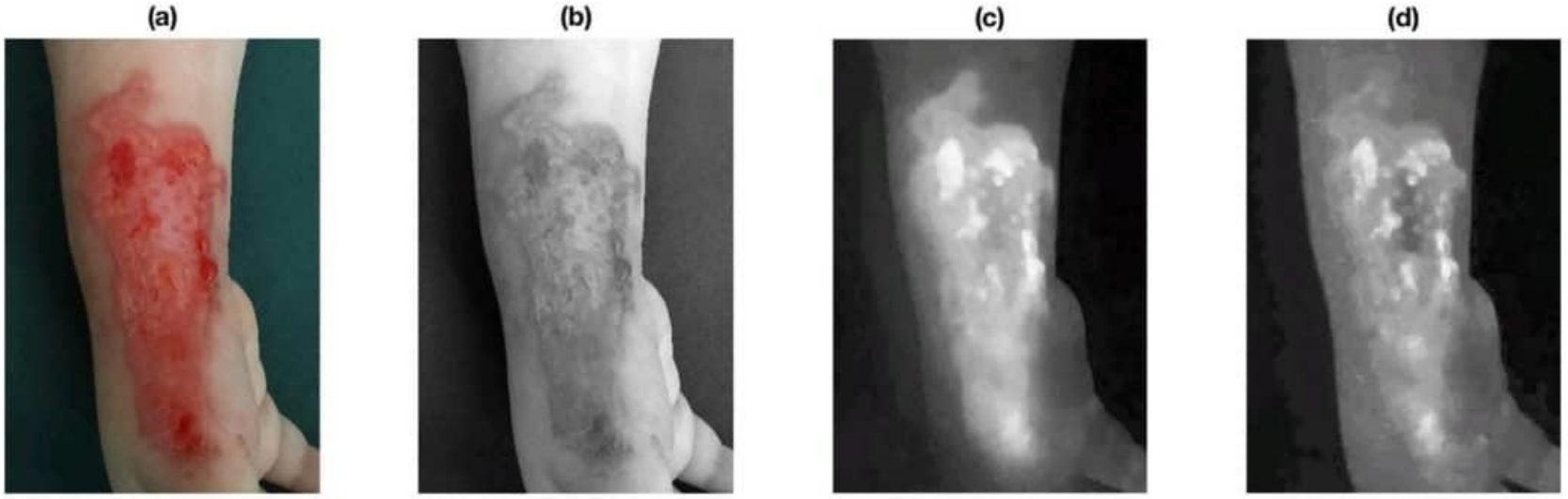

Figure 3. Burn wound colour image (**a**) and its CIELab coordinates: L^* (**b**), a^* (**c**) and b^* (**d**) respectively.

- Figures 3 and 4 show the effect of Gaussian filtering on the reduction of the reflection and producing a homogeneous background. This study does not consider the effect of illumination, which will be an issue for future investigation. Moreover, Fig. 5 shows the CIELab colour space and the CIELab tensor X for the image in Fig. 4(a).

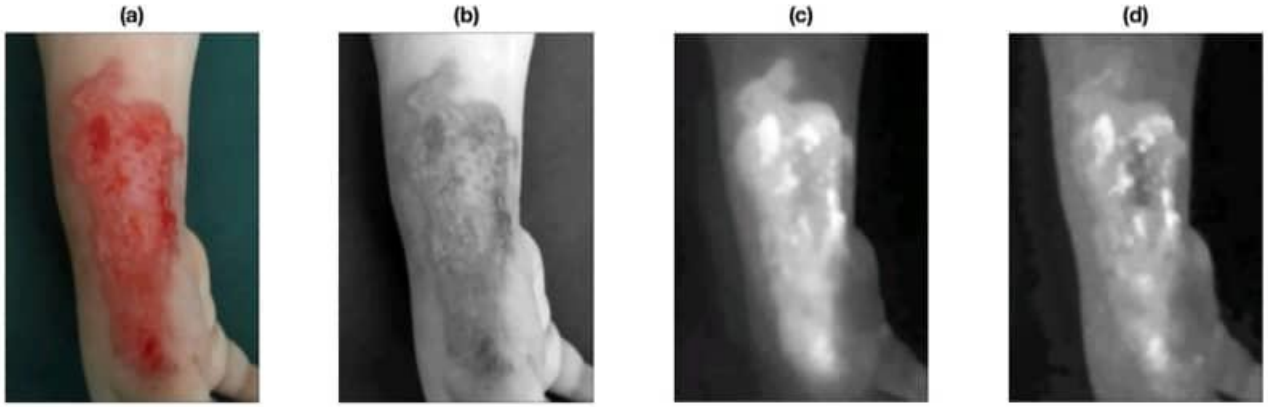

Figure 4. Burn wound colour image (**a**) and its CIELab coordinates (**b**–**d**) after Gaussian filtering in the frequency domain.

- These features were used in the FCM analysis, which initially grouped the data in 20 different clusters and successively manually merged into 3 cluster: burn wound, healthy skin and background (see Fig. 7(a)). On the other hand, Fig. 7(b) shows the final image segmentation result with the burn contour superimposed over the original image.

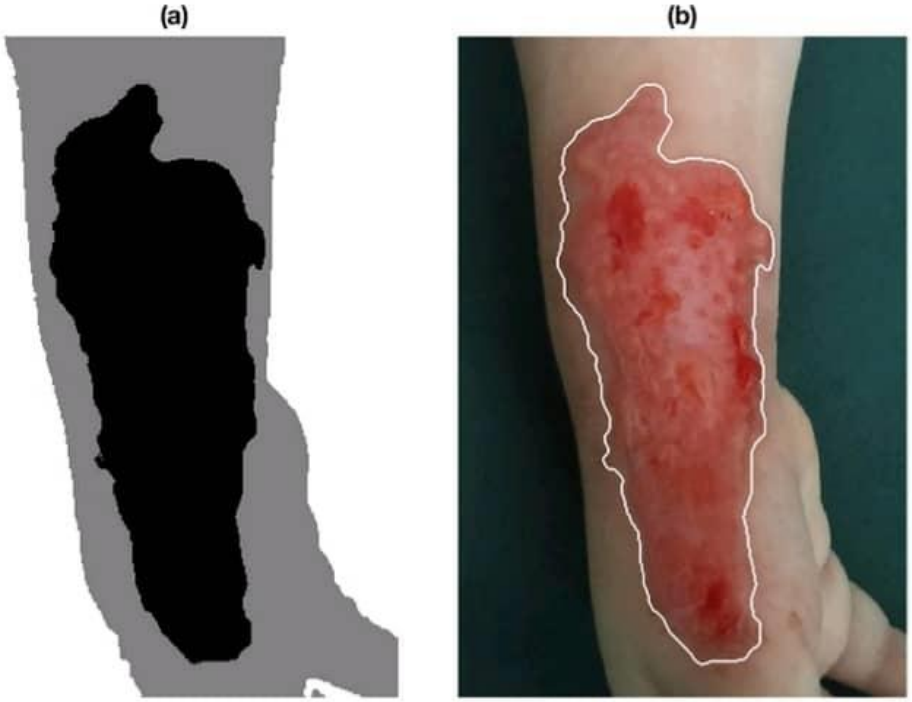

Figure 7. Result of merging of FCM clusters with the burn wound marked in black, the normal skin in grey and the background in white (**a**), and final segmentation result with the burn contour superimposed over the original image (**b**).

- In order to compare the proposed method with others, image segmentation results were obtained using four other techniques: Gaussian pre-filtering, PCA, ICA20 and the JSEG11. Figure 8 shows six segmentation results in six rows obtained from the proposed and other four methods, which are discussed as follows. It is obvious in all cases that the JSEG can only distinguish the human body from the background but not the burn wound from the healthy skin; and therefore not further included in the following comparisons.

- FIRST ROW
- For the results shown in the first row, the original image is the one discussed previously with size 1925*1330*3. The CIELab and PCA methods present under-segmented areas along the burn wound on the left side, and they took 375 and 1527 seconds for the segmentation, respectively. The ICA result is comparative with the proposed method but it required 2286 seconds for the segmentation. The proposed method successfully detects the burn wound contour after 297 seconds and using as Tucker tensor core rank: [51*38 *68].


L* a* b*
PCA
ICA
JSEG
TUCKER

- SECOND ROW
- Results in the second row involves a 1610*183*5 3 image, which shows three burn wounds after 96 hours of injury, located on the right side of the chest and in the right shoulder of a patient. The CIELab segmentation presents an over-segmentation along the upper side of the chest wound and required 493 seconds for the segmentation task. The PCA and ICA segmentation show over-segmented results along the right side of the wound in the bottom and took 1178 and 1705 seconds, respectively. The proposed method excludes the central white spot, caused by a specular reflection, from the segmentation and correctly identifies the burn wound contours in 358 seconds with Tucker tensor core rank

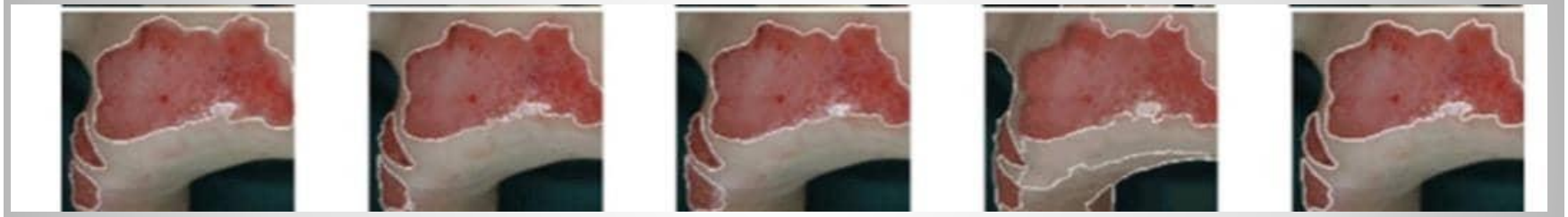

- THIRD ROW
- The third row shows segmentation results for a 1895*930*3 image of a burn wound after 17 hours of injury, located on the left side of the chest and lower left flank of a patient. CIELab segmentation resulted in over-segmentation as it joins a smaller burnt area separated by uninjured skin with the rest of the burn. At the same time, the CIELab segmentation also resulted in under-segmentation as it excluded a bit of the burnt areas on the left flank. The time taken for the CIELab is 239 seconds. The PCA and ICA present over-segmented results
- along the right side, and required 1952 and 2348 seconds for the task, respectively. The proposed method detects the burn wound contour well with a minor under-segmentation on the upper-right side of the injury in 214 seconds with Tucker tensor core rank

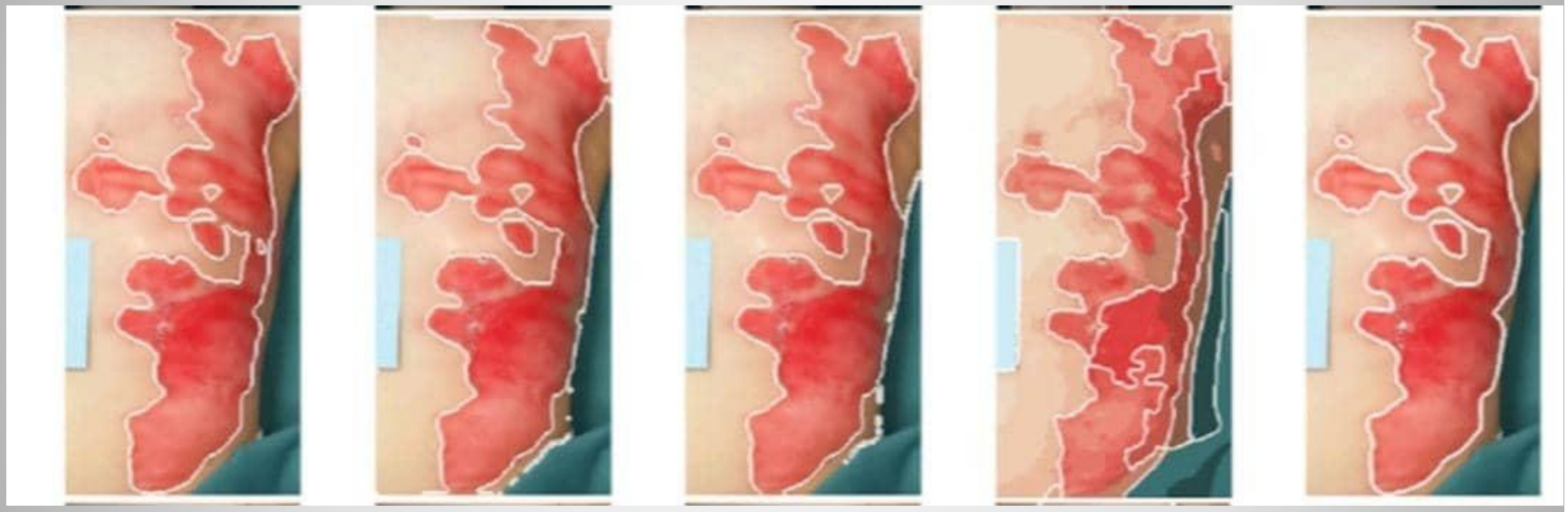

- FORTH ROW
- Segmentation results shown in the forth row for an 1505*835*3 burn image after 96 hours after injury, located next to the right ankle of a patient. Results obtained from the CIELab, PCA and ICA are similar, with over-segmentation along the left side of the image including some normal skin. These methods took 208, 800, and 3275 seconds, respectively. The proposed method detects the burn wound contour well in 118 seconds with Tucker tensor core rank

- FIFTH ROW
- The fifth row shows the segmentation results for a 965*1300*3 image of a burn wound after 312 hours of injury, located on the left forearm of a patient. The CIELab and PCA results show some minor over-segmentation on the left side, requiring 223 and 1430 seconds for the segmentation, respectively. The ICA extracted the burn area well, but it required 3653 seconds for the task. The segmentation obtained from the proposed method is similar to the CIELab and PCA methods, but only took 115 seconds for the task and Tucker tensor core rank

- SIX ROW
- The sixth row presents results for a ×× 1625 1140 3 burn image after 24 hours of injury, located on the forehead of a patient. The CIELab, PCA and ICA segmentations show noisy results caused by the reflected light and they required 308, 958 and 2824 seconds for the segmentation, respectively. Moreover, the CIELab and PCA results are of under-segmentation on the bottom-left side of the wound. The proposed method can eliminate such noise and detects the burn wound contour well in only 185 seconds with Tucker tensor core rank

- TABLE 1
- illustrates the computational times for the image segmentation obtained from different methods illustrated in Fig. 8, except for the JSEG method which produces unsatisfactory results for every images. The experimental results suggest that the proposed method can provide the best results not only in terms of segmentation accuracy but also the computational speed is approximately 10 times faster than the ICA, 5 times faster than the PCA, and 1.5 times faster than the CIELab.

Method	R1	R2	R3	R4	R5	R6	Average
CIELab	375	493	239	208	223	308	307.66
PCA	1527	1178	1952	800	1430	958	1307.5
ICA	2286	1705	2348	3275	3653	2824	2073
Proposed method	297	358	214	118	115	185	214.5

- TABLE 2
- Table 2 shows the quantitative measurements that consist of positive predicted value (PPV) and sensitivity (SEN) for a segmented image. The PPV and SEN are defined as

$$SEN = \frac{\text{The number of pixels correctly segmented by the algorithm}}{\text{The total number of pixels in the segmented region according to the expert}}$$

$$PPV = \frac{\text{The number of pixels correctly segmented by the algorithm}}{\text{The total number of pixels segmented by the algorithm}}$$

	CIELab		PCA		ICA		Tucker	
	PPV	SEN	PPV	SEN	PPV	SEN	PPV	SEN
R1	0.9366	0.9449	0.9371	0.9324	0.8848	0.9952	0.9508	0.9467
R2	0.8567	0.9767	0.9334	0.9711	0.9156	0.9853	0.9444	0.9674
R3	0.9462	0.9283	0.9018	0.9688	0.8568	0.9869	0.9478	0.9562
R4	0.8474	0.9992	0.8639	0.9967	0.8581	0.9969	0.9047	0.9953
R5	0.9666	0.9825	0.9597	0.9949	0.9936	0.9004	0.9935	0.9147
R6	0.9080	0.9795	0.9149	0.9787	0.9023	0.9916	0.9518	0.9732
Average	0.9102	0.9685	0.9184	0.9737	0.9018	0.9760	0.9488	0.9589

- For a perfect segmentation, = PPV 1 and = S 1. In case of under-segmentation, = PPV 1 and < SEN 1, whereas in case of over-segmentation, < PPV 1 and = SEN 1. Based on the results shown in Table 2, cases of under-segmentation are ICA with image R5 and Tucker with R5; and over-segmentation are CIELab with R6, PCA with R2, R3, R4, R5 and R6, ICA with R1, R2, R3, R4 and R6, and Tucker with R4.

- Both results shown in Fig. 8 and Table 2 suggest that the proposed method provides better segmentation results for the images in the 1st, 2nd, 3rd and 6th row of Fig. 8. The average PPV and SEN values of the segmentations obtained from the proposed method are better than the other three methods in terms of the balance between over-segmentation and under-segmentation

- Furthermore, the proposed method is also compared with the simple linear iterative clustering (SLIC) superpixel33, the efficient graph-based image segmentation34, and the SegNet35 methods that are discussed as follows. The SLIC super pixel method performs on the local clustering of CIELab values and pixel coordinates. It is fast and requires the specified number of super pixels as the input. Figure 9 shows the segmentation results of the original burn image as shown in Fig. 3(a) obtained from the super pixel method using 5, 20, 100, 500 and 1000 as the numbers of desired super pixels. It is quite obvious that the bigger the number of super pixels are, the better the segmentation result is obtained, but it is very difficult assign to which class a super pixel belongs to

- The algorithm distinguishes quite well the skin from the background but then encounters a problem in classifying a superpixel as skin or burn wound, resulting in either under- or over-segmentation. Being similar to the proposed method, the SLIC superpixel technique requires a manual merging process in order to distinguish the three classes of interest. However, an advantage of the proposed method over the superpixel method is that the merging process can be carried out faster since the number of clusters specified for the proposed method is much smaller than that for the SLIC superpixel technique to achieve a good final segmentation result as shown in Fig. 7(a).

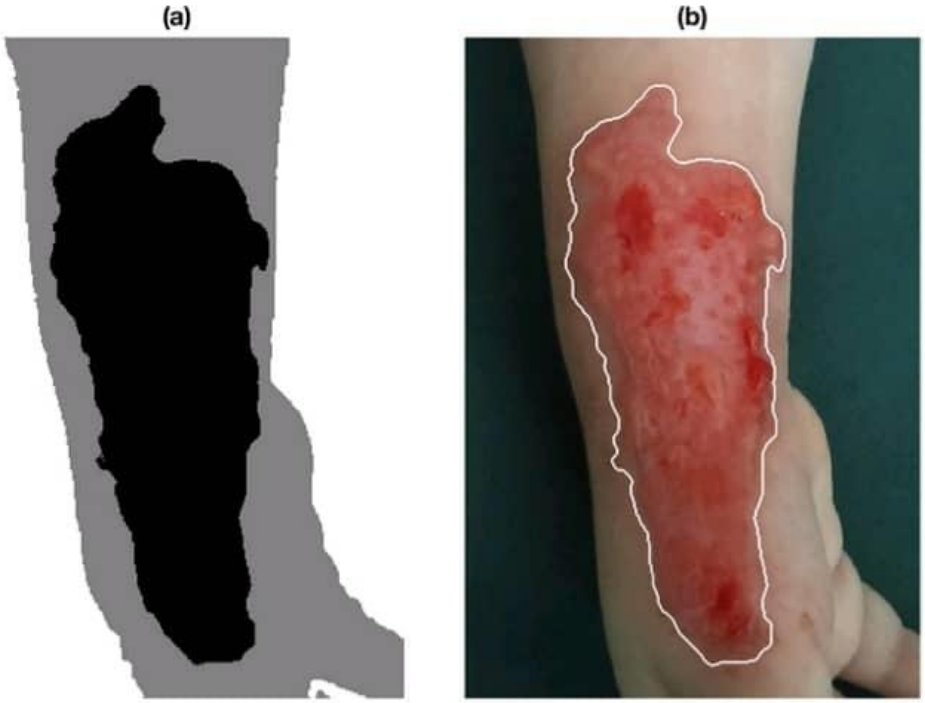

Figure 7. Result of merging of FCM clusters with the burn wound marked in black, the normal skin in grey and the background in white (**a**), and final segmentation result with the burn contour superimposed over the original image (**b**).

- The efficient graph-based image segmentation method defines a predicate to highlight the boundary between 2 or more regions using a graph-based representation of the image of interest. Figure 10 shows the segmentation results of the original burn image as shown in Fig. 3(a) obtained from the graph-based image segmentation method, where its input parameters σ =. . 05,08, and = k 100, 300, 500, 800, 1000, where σ is the standard deviation of the Gaussian filter in the pre-processing and k is a scaling parameter. It is easy to observe that all the results are not satisfactory as they were largely over-segmented.

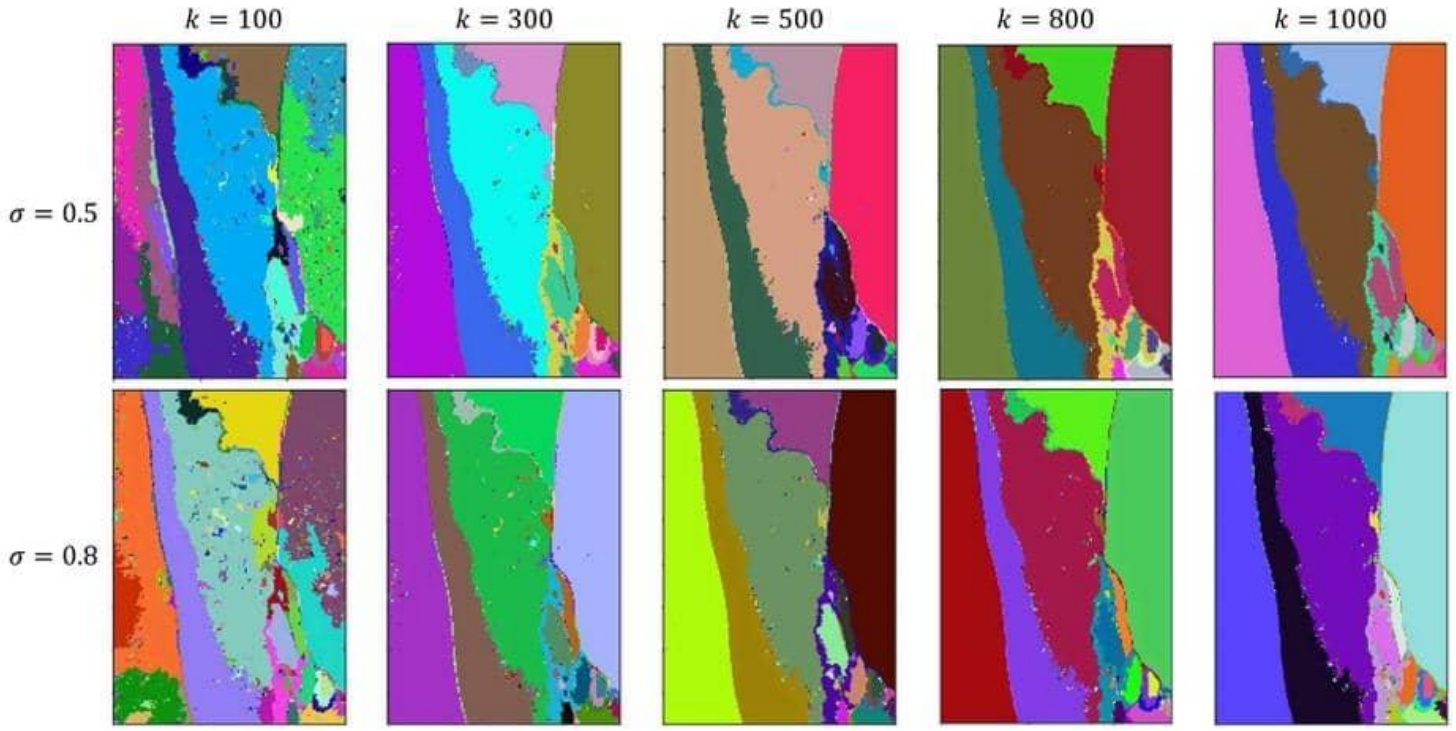

Figure 10. Efficient graph-based image segmentation results using various values of σ and k.

- **Conclusion**
- The proposed method has been shown to be able to extract burn wounds from the complex background with relatively fast computational time. The tensor decomposition is independent from the camera resolution, because it works on the CIELab tensor model instead on the number of pixels of the image. The proposed method results in a big data reduction without any information lost for the image source estimation, and therefore applicable for real-time processing. The CIELab, PCA and ICA do not consistently provide good segmentation results over various burn images, showing over/under-segmentation errors. Moreover, these techniques require longer computational times than the proposed method.

- Besides, the fuzzy burn wound centres extracted by the FCM during the cluster analysis, in this paper used to distinguish partial-thickness burns from normal skin and 1st degree burns, but they could also be used to identify the depth of the burn and classify it into: superficial partial-thickness burn, deep partial-thickness, and full-thickness burns. The 1st degree burns are not included in the total area of burn estimation and should therefore not be included in this estimation.

Thanks For Your Attention